

# SEMI-SPAN TESTING IN WIND TUNNELS

S. Eder, K. Hufnagel, C. Tropea

Chair of Fluid Mechanics and Aerodynamics, Darmstadt University of Technology

**Keywords:** *Wind Tunnel, Semi-Span, Peniche*

## Abstract

The following paper deals with the differences between full-span and semi-span testing in wind tunnels. The main objective behind this investigation was to quantify the effect of the stand-off, also known as the peniche, on the aerodynamic coefficients. To determine the influence of the peniche and to avoid disturbance between full-span and semi-span testing a new concept of a divided test-section was used.

Combined numerical and experimental studies have shown that the deviation of the aerodynamic coefficients between full-span and semi-span testing increases with increasing peniche thickness. The vortex, which develops on the wall in front of a standard two-dimensional peniche, has a major influence on the flow around the model. This is especially noticeable at the root of the wing where the separation behaviour of the flow is greatly affected. Additionally, with the two-dimensional peniche, the pressure difference between the top and bottom side of the fuselage was exaggerated. This effect explains the large deviation in the aerodynamic coefficients between the full-span and the semi-span models.

Furthermore, the present results have shown that it is beneficial to remove the peniche and to leave a gap between the model and the wall. This effectively removes the recirculation zone in front of the fuselage and the pressure difference between top and bottom side of the fuselage is equivalent to the pressure difference of the full-span model itself. These findings ultimately lead to an optimal gap size of four

times the displacement thickness of the tunnel wall boundary layer in front of the fuselage.

## 1 Introduction

Since the beginning of wind-tunnel testing of aircraft models, semi-span testing has been a common method for achieving higher Reynolds numbers while lowering the balance and model costs. The basic principle is to treat the mid-plane of the aircraft as a plane of symmetry. The mid-plane of the aircraft is mounted on the tunnel wall (or tunnel floor/ceiling) such that the tunnel wall should act as a plane of symmetry. The tunnel walls themselves are poor symmetry planes due to the growth of the respective boundary layers far upstream of the model. To avoid interactions of the tunnel boundary layer with the model, typically a stand-off, also commonly referred to as a peniche, is used between the wind tunnel wall and the half-fuselage. The most common geometry of the peniche is a two-dimensional (2d) one. A 2d peniche refers to a simple extension of the fuselage symmetry plane from the tunnel wall.

Unfortunately, previous investigations [1–9] are unsatisfactory in explaining the differences in the air flow around a full-span and a semi-span model. Furthermore, to date no universal rule about the geometry or the height of the peniche exists. One major obstacle with earlier experiments was that comparisons between semi-span and full-span testing were often performed in different wind tunnels or with different aircraft models. Prior numerical simulations neglected to model the flow between the fuselage and the peniche (e.g. in the

labyrinth sealing). The many short-comings of prior experimental and numerical efforts listed above, have attempted to be addressed in the current investigation.

## 2 Experimental and numerical setup

The peniche geometry and its subsequent optimization are the major topics of the present investigation. To avoid the challenges of using different tunnels and varying support geometries, the experimental studies have been performed using an entirely new concept. This concept includes a wall to divide the test section of the wind tunnel, incorporating a specially built model which can be used as a full-span model or as two semi-span models. With this concept, full-span and semi-span tests were performed using identical models in exactly the same wind tunnel and at exactly the same position. The only discrepancy between both full- and semi-span configurations is the additional blockage (1.3%) of the mid-wall.



Fig. 1: Full-span configuration in the test section

This semi-span arrangement is not typical, but it is an ideal arrangement to examine the influence of the peniche on the flow pattern and the associated aerodynamic coefficients. For the full-span tests, the model was connected to the external balance under the test-section with vertical supports. Similarly, for the semi-span tests, the same balance and supports were used. Inside the mid-wall the semi-span models were connected with a shaft,

i.e. the forces on both semi-span models were measured combined.

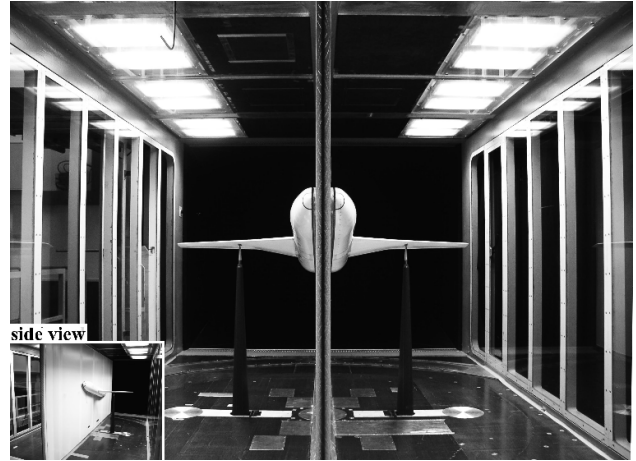


Fig. 2: Semi-span configuration in the divided test section

The model used for all tests was a 2.28m-long wing-fuselage combination without tail unit. The tests were performed at three Reynolds numbers ( $Re = 5.90 \times 10^5$ ,  $7.58 \times 10^5$  and  $9.26 \times 10^6$ ) related to the mean chord length. The pressure distribution was measured in a plane 15mm from and parallel to the symmetry plane. During the semi-span experiments, the pressure was measured on one side of the mid-wall along a line extending from the leading edge to the trailing edge of the wall. This line intersects the nose of the fuselage and runs parallel to the floor of the test-section, and was used to determine the pressure gradient along the wall, especially in front of the fuselage itself. To check for flow symmetry on both sides of the test-section, the pressure was measured at several points on the opposing side of the mid-wall. The flow was also visualized with tufts. The measurements of the boundary layer at the mid-wall reveal a displacement thickness in front of the fuselage of  $\delta^* = 3\text{mm}$ . The boundary-layer thickness at the same position is  $\delta = 24\text{mm}$ .

As the reference case for all semi-span experiments, the full-span configuration tests were conducted at the three Reynolds numbers. Subsequently, the semi-span tests were performed at the same Reynolds numbers. For semi-span tests with the 2d-peniche, four peniche thicknesses  $1\delta^*$ ,  $2\delta^*$ ,  $6\delta^*$  and  $10\delta^*$

were used. Between the peniche and the fuselage, a labyrinth seal was inserted. The investigations without the peniche were performed with gap sizes of  $2\delta^*$ ,  $4\delta^*$ ,  $6\delta^*$ ,  $8\delta^*$  and  $10\delta^*$ . The symmetry plane of the fuselage was closed with a 2mm-thick steel sheet. The sheet was connected to the model, so that the forces on the surface of the sheet were included in the measurements. The shaft connecting the two semi-span models was also enclosed with a fairing.

The following additional corrections were made to all results of the semi-span tests: a) additional blockage of the wall; b) additional blockage of the peniche; c) higher aspect ratio due to the mid-wall and the peniche.

Prior to the wind tunnel tests, the experimental setup was numerically simulated. The numerical simulations were used to pre-select peniche-geometries and to visualize the flow. Hence, only a brief comparison of the numerical results will be shown here. Fig. 3 shows the calculated geometries. The 2d-peniche was calculated with a peniche thickness of  $2\delta^*$ ,  $6\delta^*$ ,  $8\delta^*$  and  $10\delta^*$ . With the additional trench the peniche thicknesses of  $6\delta^*$  and  $10\delta^*$  were calculated. With the mirrored fuselage two peniches were simulated;  $20\delta^*$  and  $40\delta^*$  (fuselage radius =  $40\delta^*$ ) and the configuration without peniche was calculated with a gap size of  $6\delta^*$ ,  $8\delta^*$  and  $10\delta^*$ . Fig. 3 also shows the shaft within the gap. This shaft connects both semi-span models through the mid-wall.

In Fig. 4, some of the results of the numerical simulation are depicted. The graph shows that with a 2d-peniche or a mirrored fuselage, the deviation of the lift coefficient between the semi-span configuration and the full-span configuration increases with increasing peniche thickness. With the 2d-peniche plus trench configuration, the deviation is almost constant. Without the peniche, however, there is almost no deviation between the full-span and the semi-span configurations. Hence, the experimental setup for the semi-span testing was performed with 2d-peniches of varying peniche thickness (currently a 2d-

peniche is standard in wind tunnel testing) and without a peniche but with a gap between the fuselage and the wall.

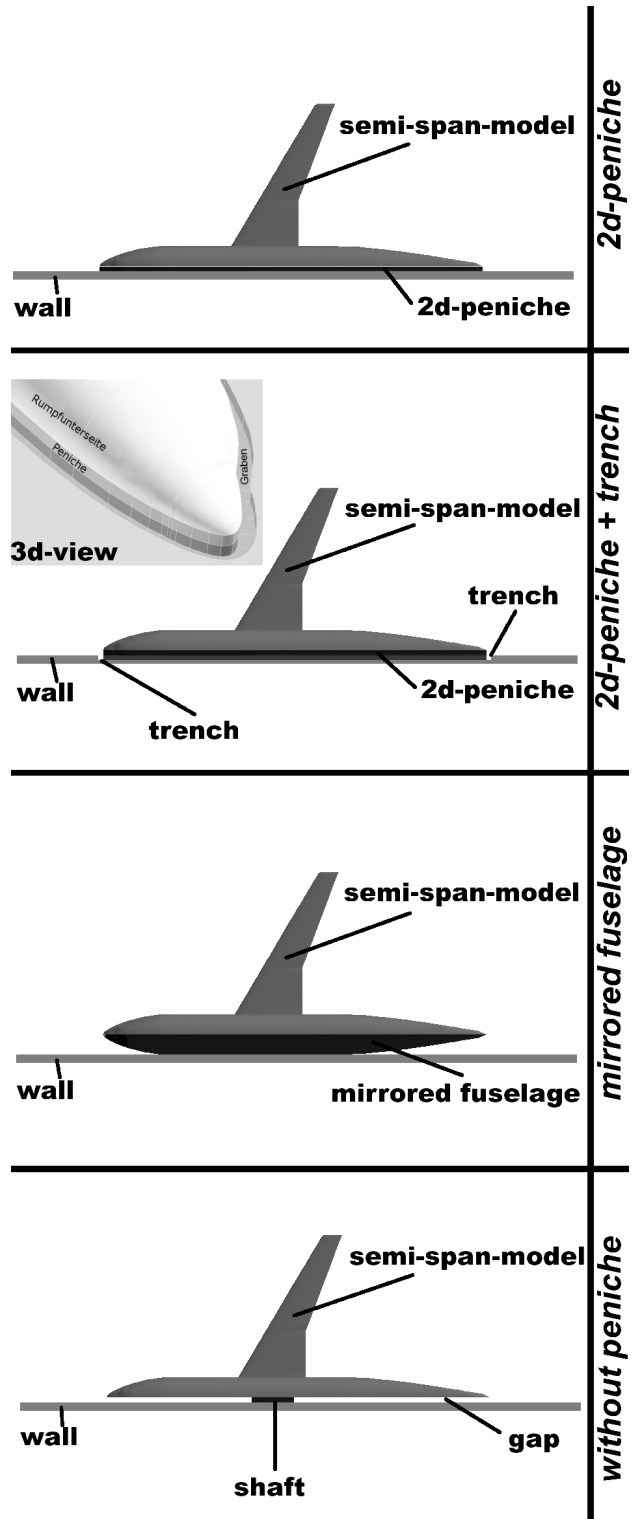


Fig. 3: Numerically calculated geometries

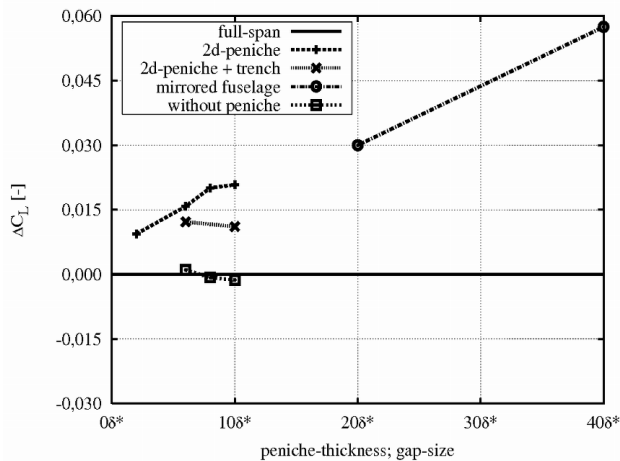


Fig. 4:  $\Delta C_L$  between full-span and semi-span configurations at  $\alpha = 6^\circ$  and  $Re = 590000$

### 3 Results

The results of the full-span tests show a slightly varying behaviour in the aerodynamic coefficients (Fig. 5) for the different Reynolds numbers. However, at all three Reynolds numbers, the lift coefficient is linear between angles of attack of  $-5^\circ$  and  $+4^\circ$ . The maximum lift occurs at an angle of attack of approximately  $13^\circ$ . Due to the missing tail unit, the moment coefficient is not constant with angle of attack, and at positive angles of attack, the model was found to be tail-heavy.

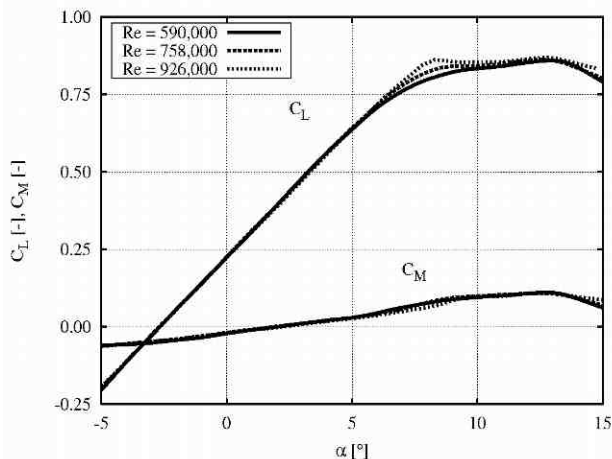


Fig. 5: Lift and moment coefficient of the full-span configuration

The separation of the flow at the model starts on the top side of the wing if the angle of attack is greater than  $4^\circ$ . The first signs of separation occur at the trailing edge (Fig. 6 section (1)). Afterwards, section (2) near the

root of the wing separates. With further increases in angle of attack, from the wing tip and from the sections (1) and (2) the separation extends through section (3), to section (4). At  $9^\circ$  the whole of section (3) has separated. Then, with a slight increase in angle of attack, section (4) separates abruptly. Finally, at  $15^\circ$  angle of attack, section (5) is also separated. The difference in the separation pattern as a function of Reynolds number is the size of section (4). With increasing Reynolds numbers, section (4) is larger and the growth of separation in section (3) slower.

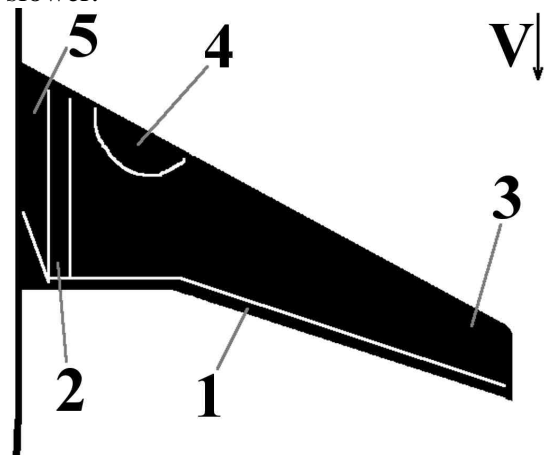


Fig. 6: Sketch of the separation behavior at the top side of the wing

#### 3.1 Lift Coefficient

The comparison between the full-span tests and the semi-span tests shows a very interesting behaviour in the gradient of the lift coefficient in the linear part of the  $C_L$ - $\alpha$  graph. With the 2d-peniche, the gradient is higher than the gradient of the full-span configuration. Furthermore, this gradient is found to increase with increasing peniche thickness. On the other hand, the semi-span experiments without peniche produce a decreasing gradient with increasing gap size, and between  $4\delta^*$  to  $6\delta^*$ , the gradient is the same as the gradient of the full-span model. This behaviour was found to be independent of the Reynolds number.

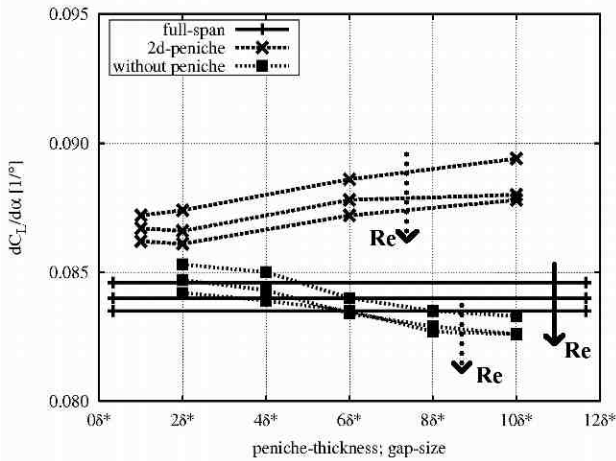


Fig.6 Lift gradient as a function of the peniche-thickness/gap-size

The 2d-peniche tests highlight two major differences with respect to the full-span model. First, the flow pattern at the top-side of the wing is altered, and secondly, the pressure difference between the top and the bottom sides of the fuselage is exaggerated. In Fig. 7, the pressure difference is nearly equal for the different models up to the start of separation on the fuselage (angle of attack of 6°). Fig. 7 depicts the pressure differences as a function of the angle of attack at  $x/l_{fuselage} = 0.5521$ .

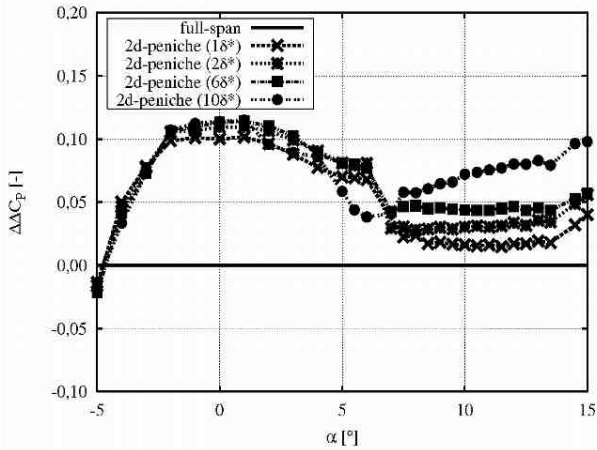


Fig. 7 Pressure difference between bottom and top sides of the fuselage for semi-span with 2d-peniche and full-span configurations ( $x/l_{fuselage} = 0.5521$ )

Fig. 8 and Fig. 9 show the flow on top of the wing at an angle of attack of 7°. For the full-span configuration, the rear of the inboard wing contains a more separated flow than with the semi-span configuration (with 2d-peniche). This is a result of the vortex created in front of the nose. This vortex forms a horseshoe shape

around the fuselage. The numerical simulations have revealed that some parts of the vortex interact with the inboard wing (Fig. 10). This in turn increases the turbulence in the flow inboard of the wing and leads to a delayed separation. Hence, the lift coefficient is higher for the semi-span model.

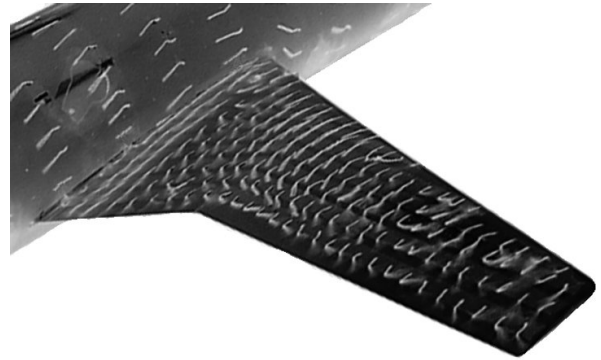


Fig.8 Flow on the top side of the wing (full-span;  $\alpha = 7^\circ$ )

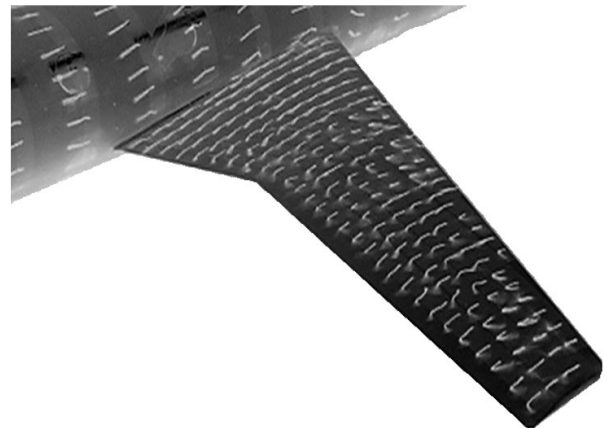


Fig. 9: Flow on the top side of the wing (semi-span; 2d-peniche;  $\alpha = 7^\circ$ )

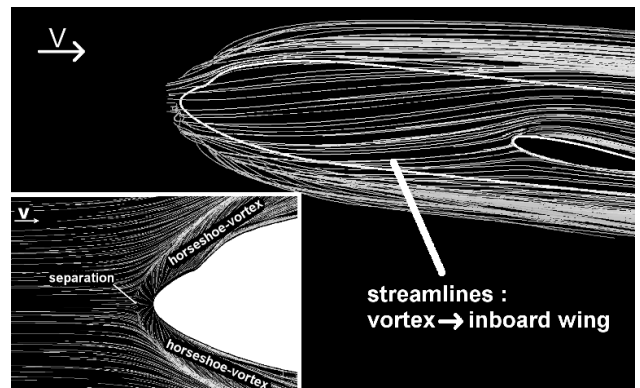


Fig. 10: Streamlines at the fuselage (numerical simulations)

In contrast to the 2d-peniche, the configurations without a peniche show a decrease in lift gradient with increasing gap size. The primary cause of the smaller gradient is the flow in the gap between the fuselage and the wall. This flow can be seen as an additional circulation around the fuselage (Fig. 11). This circulation leads to an increase in angle of attack at the wing. With an increase in distance between the fuselage and the wall, the flow in the gap increases. Thus, the circulation around the fuselage is higher along with the induced angle of attack.



Fig. 11: Additional circulation around the fuselage

A second major difference between both semi-span configurations (2d-peniche and without peniche) is the flow pattern inboard of the wing. With the 2d-peniche, the flow separates later than in the full-span configuration. However, there is only a small difference in the flow pattern between the full-span configuration and the semi-span configuration without a peniche (Fig. 8 vs. Fig. 12). As a result, the tests without peniche produce a lower pressure gradient at the wall in front of the fuselage as with the 2d-peniche. Therefore, due to the acceleration of the flow into the gap, the flow doesn't separate from the wall. Hence, no vortex is created which could potentially influence the flow inboard of the wing.

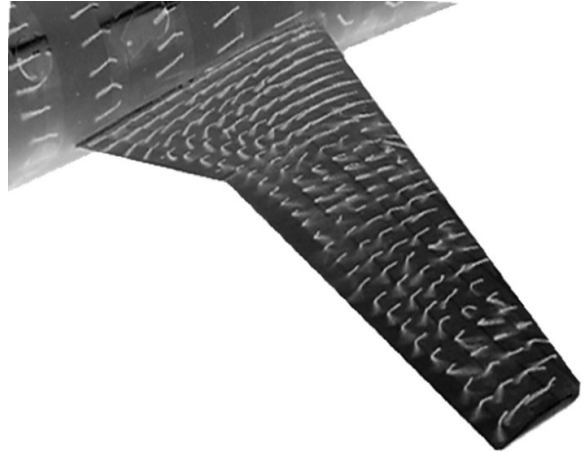


Fig. 12: Flow over the top side of the wing (semi-span; 2d-peniche;  $\alpha = 7^\circ$ )

The final major difference between the 2d-peniche configuration and the configuration without peniche is the pressure difference between the top and the bottom sides of the fuselage. Fig. 13 shows that the pressure difference without peniche is nearly equal to the pressure difference of the full-span model, contrary to the semi-span model with the 2d-peniche (Fig. 7).

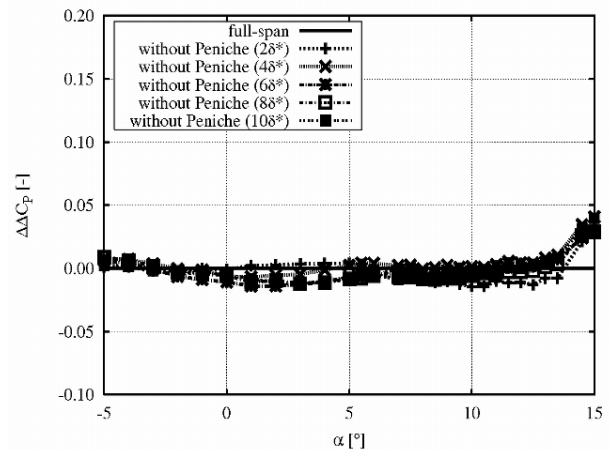


Fig. 13: Pressure difference between bottom and top side of the fuselage and between semi-span without peniche and full-span configuration ( $x/l_{\text{fuselage}} = 0,3007$ )

However, Fig. 13 also shows that with increasing distance between the fuselage and the wall, the pressure difference decreases due to the increase in flow within the gap. One disadvantage of the configuration without peniche is depicted in Fig. 14. Here the pressure difference between the bottom and top sides of the fuselage at  $x/l_{\text{fuselage}} = 0.5521$  is greatly

influenced by the wake of the shaft between the wall and the model itself.

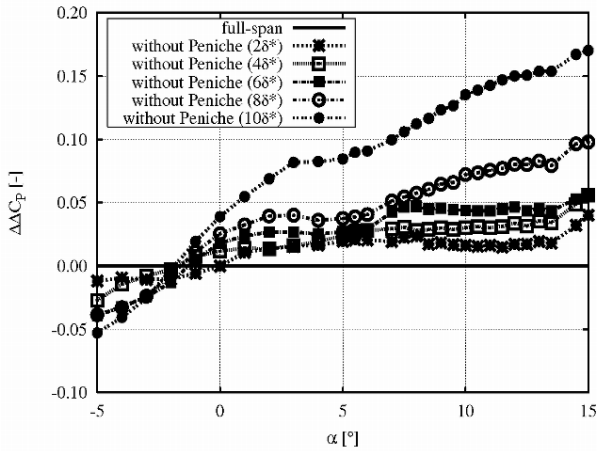


Fig.14: Pressure difference between bottom and top sides of fuselage for semi-span without peniche and full-span configurations ( $x/l_{fuselage} = 0.5521$ )

With higher angles of attack the shaft wake moves more and more to the top side of the fuselage and influences the pressure in the region. This is clearly depicted in Fig. 15. Here the model angle of attack is  $6^\circ$  whereas the wake angle of attack is  $-20^\circ$ . With a  $0^\circ$  model angle of attack, the wake angle of attack is approximately  $-3^\circ$ . Fig. 14 also shows that the influence of the wake is less for smaller gaps.

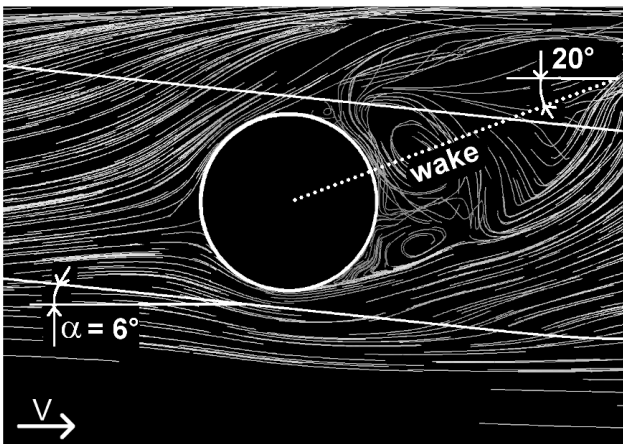


Fig. 15: Streamlines in the gap between fuselage and wall (gap size =  $10\delta^*$ , numerical simulations)

### 3.2 Drag Coefficient

Fig. 16 and Fig. 17 show the deviation of the drag coefficient between semi-span and full-span configurations as a function of angle of attack. The comparison of the full-span model

with the semi-span configurations shows that the drag coefficient of the 2d-peniche configuration is nearly equal to the drag coefficient of the full-span model. This is the case up to the start of the separation over the wing. However once separation has begun, the deviation in drag decreases due to the delayed separation inboard of the wing. Only the drag deviation for the largest peniche increases. But here the flow pattern at the fuselage changes, because the peniche is now thicker than the boundary layer. For all peniche thicknesses the deviation in the drag coefficient was found to be a function of the angle of attack.

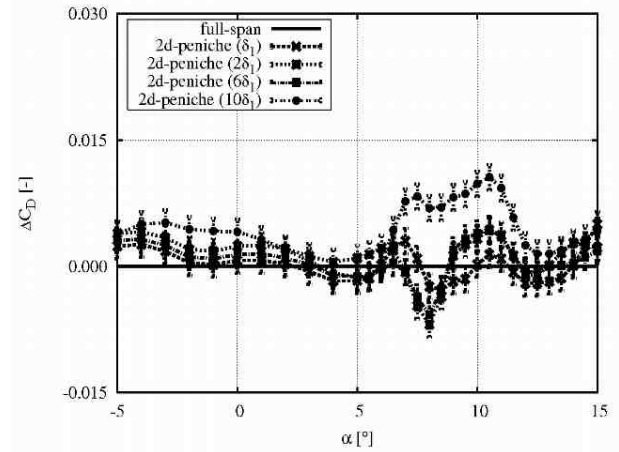


Fig. 16: Difference in drag coefficient between semi-span for 2d-peniche and full-span configurations ( $Re = 758000$ )

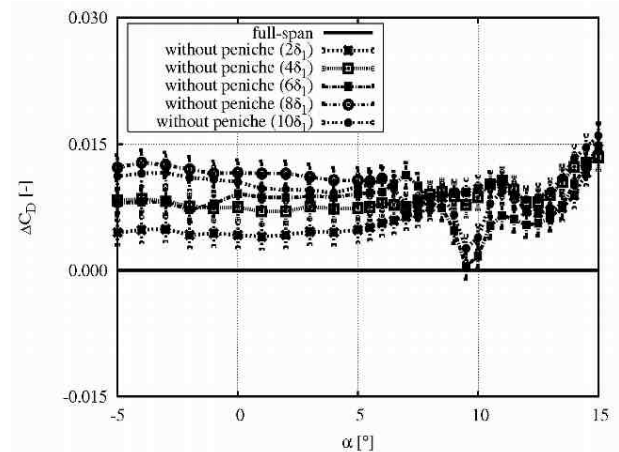


Fig. 17: Difference in drag coefficient between semi-span without peniche and full-span configurations ( $Re = 758000$ )

Fig. 17 shows that the drag coefficient of the semi-span configuration without peniche is

much higher than the drag coefficient of the full-span configuration. Between angles of attack of  $-5^\circ$  to  $+4^\circ$  (linear part of lift curve) the deviation is a function of the distance between the fuselage and the wall. However, within this same range of angles of attack (for all gap sizes), the deviation of the drag coefficient is constant and not a function of the angle of attack itself. This result is an almost constant offset to the full-span configuration. The offset increases with increasing gap size. Only with the onset of separation at the wing does the deviation begin to vary for the big gap sizes. However, with the gap size of  $4\delta^*$ , the deviation is constant between  $-5^\circ$  and  $+13^\circ$ .

There are two causes for the higher drag without peniche. The main cause is the flow over the symmetry plane of the fuselage. As described, the symmetry plane was closed with a 2mm-thick steel sheet, which was in turn connected to the fuselage. Hence, the friction that occurs over the sheet results in the higher drag of the model. The flow in the gap increases with increasing gap size, thus the associated drag increases too. The other cause for the higher drag is the effect of the shaft-wake on the afterbody of the fuselage. Despite the disadvantage of higher drag, the test configuration without peniche offers a large advantage, that the deviation is not a function of the angle of attack over a wide range.

### 3.3 Moment Coefficient

Fig. 18 and Fig. 19 show the deviation of the moment coefficients between semi-span and full-span configurations as a function of the angle of attack. The moment coefficients as a function of the angle of attack show a similar behaviour to the drag coefficient, except for the high offset without peniche. The offset in the moment coefficient is, however, smaller. The deviation of the moment coefficient between the semi-span configurations with 2d-peniche and the full-span model varies with the angle of attack. Without a peniche the deviation is almost constant. For example, the deviation for a gap size of  $4\delta^*$  is constant for angles of attack between  $-5^\circ$  and  $+8^\circ$ . Only at higher angles of

attack does the deviation vary (increasing with angle of attack). Similarly the deviation for the 2d-peniche case increases with increasing angle of attack. Again the configuration without peniche is found to be beneficial, as compared to the 2d-peniche configuration, because the moment coefficient is more stable throughout the range of angles of attack.

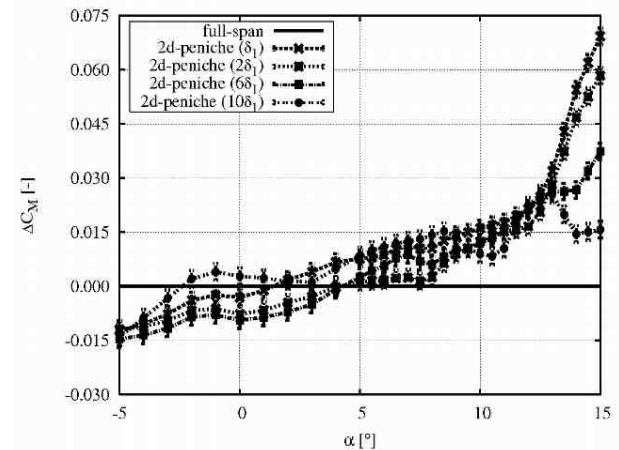


Fig. 18 Difference in moment coefficients for semi-span with 2d-peniche and full-span configurations ( $Re = 758000$ )

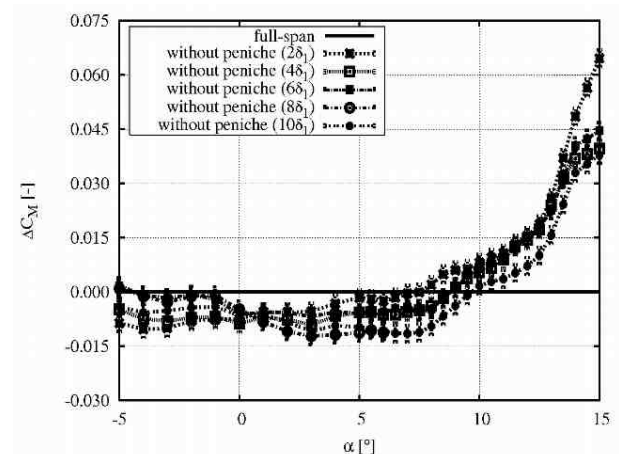


Fig. 19 Difference in moment coefficient for semi-span without peniche and full-span configurations ( $Re = 758000$ )

## 4 Conclusions

The results of this investigation prove that semi-span testing without peniche leads to more consistent results than with a 2d-peniche. A 2d-peniche generates a vortex in front of the fuselage at the wall, which in turn influences the flow pattern inboard of the wing, creating a delayed separation. Furthermore, the pressure

differences between the bottom and the top sides of the fuselage is exaggerated with the 2d-peniche. The 2d-peniche tests had aerodynamic coefficient deviations ranging between the full-span and the semi-span-configurations but were strongly influenced by the angle of attack. Without peniche and gap between the fuselage and the wall, the deviations were almost independent of the angle of attack, especially prior to separation. Only at high angles of attack, at which point the flow was completely separated, were the deviations of both semi-span configurations too large.

The best results were obtained without a peniche and for a gap size of  $4\delta^*$ . For this optimal distance of  $4\delta^*$  between the fuselage and the wall, the deviations of the aerodynamic coefficients to the full-span configuration were constant (stable) over a broad range of angles of attack.

## 5 Outlook

Further research should focus on high-lift configurations at low-Reynolds numbers to determine the influence of much higher pressure differences on the gap. Also of interest would be tests on a clean wing at higher Reynolds numbers or variations of the connecting shaft geometry, i.e. streamlining. Finally, changes to the model construction should be made, such that the steel sheet is decoupled from the fuselage. In this manner the additional frictional forces generated by the sheet would not be measured.

## References

- [1] Earnshaw, P.B.; Green, A.R.; Hardy, B.C., Jelly, A.H.; A Study of the Use of Half-Models in High-Lift Wind-Tunnel Testing; Defence Research Agency, Controller HMSO, London, 1992
- [2] Gatlin, G.M.; McGhee, R.J.; Study of Semi-Span Model Testing Techniques; AIAA 96-2386, 1996
- [3] Gatlin G.M.; Parker P.A., Owens Jr., L.R.; Advancement of Semispan Testing at the National Transonic Facility; Journal of Aircraft, Vol.39, No.2, March – April 2002
- [4] Gatlin G.M.; Parker P.A., Owens Jr., L.R.; Development of a Semi-Span Test Capability at the National Transonic Facility; AIAA-2001-0759
- [5] Krynytzky, A.J.; Steady-State Wall Interference of a Symmetric Half-Model in the Langley Transonic Dynamics Tunnel; AIAA 2001-0161
- [6] Marchman, J.F.; Gunther, C.L.; Gundlach, J.F.; Semi-Span Testing at low Reynolds Number; AIAA 98-0608
- [7] Milholen II, W.E.; A Design Methodology for Semi-Span Model Mounting Geometries; AIAA 98-0758
- [8] Milholen II, W.E.; Chokani, N.; McGhee, R.J.; Development of Semi-Span Model Test Techniques; AIAA 96-2412, 1996
- [9] Milholen, W.E., Chokani, N.; Computational analysis of semi-span model test techniques; NASA CR 4709, 1996
- [10] Mokry, M.; Khalid, M.; Wind Study of Transonic Wall Interference in Two-Dimensional Wind Tunnels; AIAA 2000-2375